JCB Article

Dynamic redistribution of raft domains as an organizing platform for signaling during cell chemotaxis

Concepción Gómez-Moutón, Rosa Ana Lacalle, Emilia Mira, Sonia Jiménez-Baranda, Domingo F. Barber, Ana C. Carrera, Carlos Martínez-A., and Santos Mañes

Department of Immunology and Oncology, Centro Nacional de Biotecnología (CNB)/CSIC, UAM Campus de Cantoblanco, E-28049 Madrid, Spain

Spatially restricted activation of signaling molecules governs critical aspects of cell migration; the mechanism by which this is achieved nonetheless remains unknown. Using time-lapse confocal microscopy, we analyzed dynamic redistribution of lipid rafts in chemoattractant-stimulated leukocytes expressing glycosyl phosphatidylinositol–anchored green fluorescent protein (GFP-GPI). Chemoattractants induced persistent GFP-GPI redistribution to the leading edge raft (L raft) and uropod rafts of Jurkat, HL60, and dimethyl sulfoxide–differentiated HL60 cells in a pertussis toxin–sensitive, actin-dependent manner. A transmembrane, nonraft GFP protein was distributed homogeneously in moving cells. A GFP-CCR5 chimera, which partitions in L rafts, accumulated at the leading edge, and CCR5 redistribution coincided with recruitment and activation of phosphatidylinositol-3 kinase γ in L rafts in polarized, moving cells. Membrane cholesterol depletion impeded raft redistribution and asymmetric recruitment of PI3K to the cell side facing the chemoattractant source. This is the first direct evidence that lipid rafts order spatial signaling in moving mammalian cells, by concentrating the gradient sensing machinery at the leading edge.

Introduction

Migrating cells must integrate spatial and temporal information provided by environmental cues through acquisition of a polarized morphology (Lauffenburger and Horwitz, 1996). This functional segregation is possible because cells restrict the activation and amplification of distinct sets of signaling pathways in specific cell areas. Evidence from Dictyostelium suggests that differential localization of PI3K (at the leading cell edge) and PTEN (at the uropod) are key factors in forming the robust internal gradients required for chemoattractant sensing and directed cell movement (Funamoto et al., 2002; Iijima and Devreotes, 2002). In mammalian cells, an asymmetrical internal PI(3,4,5)P_3 gradient is formed during cell chemotaxis (Servant et al., 2000). There is nonetheless controversy as to whether chemosensory receptors polarize in migrating cells (Sullivan et al., 1984; Walter and Marasco, 1984; McKay et al., 1991; Nieto et al., 1997; Mañes et al., 1999, 2003b; Servant et al., 1999; Gómez-Moutón et al., 2001; Zhao et al., 2002; Katagiri et al., 2003; van Buul et al., 2003). Identification of the mechanisms that localize and restrict signaling activation in chemotaxing cells thus remains a central question.

Membrane rafts have been characterized as cholesterol- and glycosphingolipid-enriched domains. A role is proposed for rafts in cell migration based on the observation that depletion of plasma membrane cholesterol inhibits cell polarization and migration (Mañes et al., 1999; Khanna et al., 2002). Asymmetric raft domain distribution has also been described after cell stimulation with chemoattractants or with electric fields (Mañes et al., 1999; Gómez-Moutón et al., 2001; Seveau et al., 2001; Millan et al., 2002; Zhao et al., 2002; van Buul et al., 2003). In some reports, this redistribution parallels chemoattractant receptor accumulation at the leading edge (Mañes et al., 1999; Gómez-Moutón et al., 2001; Zhao et al., 2002; van Buul et al., 2003), raising the possibility that rafts act as signal amplification centers during cell polarization and chemotaxis. Uropod raft accumulation

C. Gómez-Moutón and R.A. Lacalle contributed equally to this work.

The online version of this article contains supplemental material.

Address correspondence to Santos Mañes, Dept. of Immunology and Oncology, Centro Nacional de Biotecnología/CSIC, UAM Campus de Cantoblanco, E-28049 Madrid, Spain. Tel.: 34-91-585-4660. Fax: 34-91-372-0493. email: smanes@cnb.uam.es

Key words: cell polarization; lipid rafts; chemotaxis; chemokine; phosphatidyl inositol-3 kinase

Abbreviations used in this paper: CD, cyclodextrin; CTx, cholera toxin β-subunit; cytRFP, cytosolic red fluorescent protein; DRM, detergent-resistant membranes; L raft, leading edge raft; PH, pleckstrin homology; PHAKT-GFP, AKT PH domain fused to GFP; PHAKT-RFP, AKT PH domain fused to DsRed2-FP; PI3Kγ, phosphatidylinositol-3 kinase γ; PTx, pertussis toxin; U raft, uropod raft.

The Journal of Cell Biology, Volume 164, Number 5, March 1, 2004 759–768
http://www.jcb.org/cgi/doi/10.1083/jcb.200309101

The Journal of Cell Biology

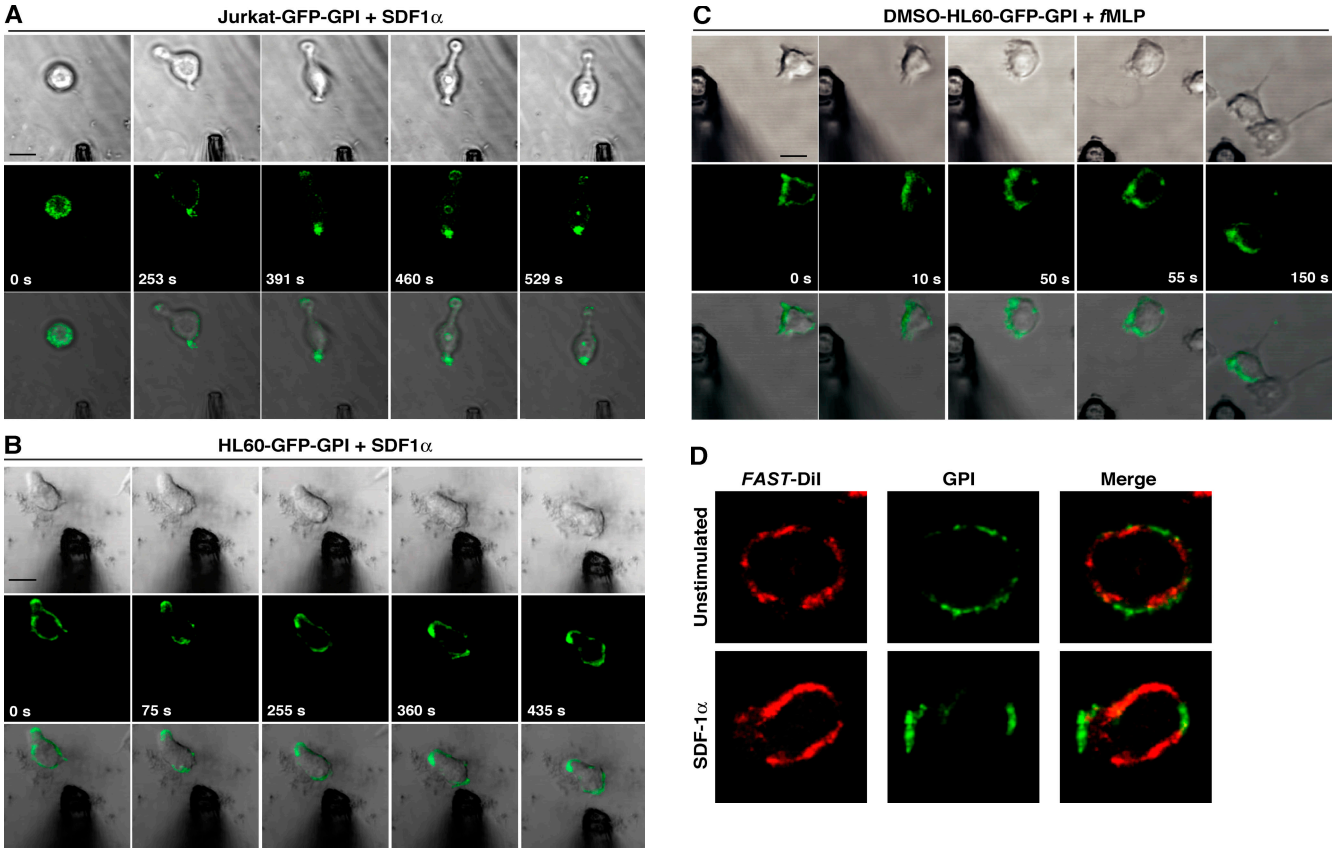

Figure 1. **Leukocytes redistribute L and U rafts during chemotaxis.** (A) Chemotaxis assays were performed by placing an SDF-1α–loaded micropipette near Jurkat cells expressing GFP-GPI; the gradient was formed by passive diffusion of the chemoattractant. Dark-phase and green fluorescence were recorded in a confocal microscope at 23-s intervals. The pipette tip is observed at center bottom. (B) GFP-GPI–expressing HL60 cells were examined in chemotaxis assays using an SDF-1α–loaded pipette; images were recorded every 15 s. Pipette position was changed during the recording period. (C) HL60-DMSO cells were analyzed for chemotaxis toward an *f*MLP-loaded pipette. The first 15 frames were recorded at 5-s intervals and remaining frames every 20 s. Cells in A–C are representative of 40 of 46, 29 of 30, and 31 of 31 cells, respectively; animated versions of these figures are provided as online supplemental material (available at http://www.jcb.org/cgi/content/full/jcb.200309101/DC1). (D) Jurkat cells were prelabeled on ice with *FAST*-DiI, then plated onto fibronectin-coated coverslips and stimulated or not with SDF-1α. After 10 min, cells were imaged directly by confocal microscopy. Bars, 10 μm.

is also reported for T cells (Millan et al., 2002) and neutrophils (Seveau et al., 2001). In Jurkat cells, raft subtypes distinguished by ganglioside composition have been identified at each cell pole, with leading edge rafts (L rafts) enriched in GM3, whereas uropod rafts (U rafts) are GM1-enriched (Gómez-Moutón et al., 2001). The evidence for asymmetric raft distribution was obtained in fixed cells; it is consequently not known whether rafts in fact redistribute during directional cell movement.

Here, we used time-lapse confocal microscopy to analyze the dynamic redistribution of raft domains in chemoattractant-stimulated leukocytes. We found that chemoattractants induce persistent redistribution of raft-associated glycosylphosphatidyl inositol (GPI)–anchored GFP (GFP-GPI) to both cell edges in a pertussis toxin (PTx)–sensitive, actin-dependent manner, confirming L and U raft segregation in polarized leukocytes. The implication of raft reorganization in signaling was studied by analyzing chemoattractant receptor redistribution in chemotaxing cells. We observed that CCR5 redistributed preferentially to the leading edge of polarized migrating cells. This chemoattractant receptor accumulation correlates with phosphatidylinositol-3 kinase γ (PI3Kγ) recruitment to L rafts, where it is subsequently activated, as determined by AKT pleckstrin homology (PH) domain recruitment in chemotaxing cells. The results indicate that lipid rafts are platforms for organize spatial signaling during cell chemotaxis, and constitute the first direct evidence of PI3Kγ polarization in chemotaxing mammalian cells.

Results

Raft-associated proteins redistribute to both cell poles during leukocyte chemotaxis

Using high resolution single particle tracking, it was shown that GPI-anchored proteins neither leave nor are laterally displaced from lipid rafts (Pralle et al., 2000). We analyzed raft redistribution during cell chemotaxis by studying relocation of the GFP-GPI protein expressed in distinct cell types (unpublished data). When GFP-GPI–expressing Jurkat (Fig. 1 A; Video 1, available at http://www.jcb.org/cgi/content/full/jcb.200309101/DC1), HL60 (Fig. 1 B; Video 2), and HL60–dimethyl sulfoxide (DMSO) cells (Fig. 1 C; Video 3) were exposed to SDF-1α (Jurkat and HL60 cells) or to *N*-formyl-Met-Leu-Phe (*f*MLP; HL60-DMSO cells), GFP

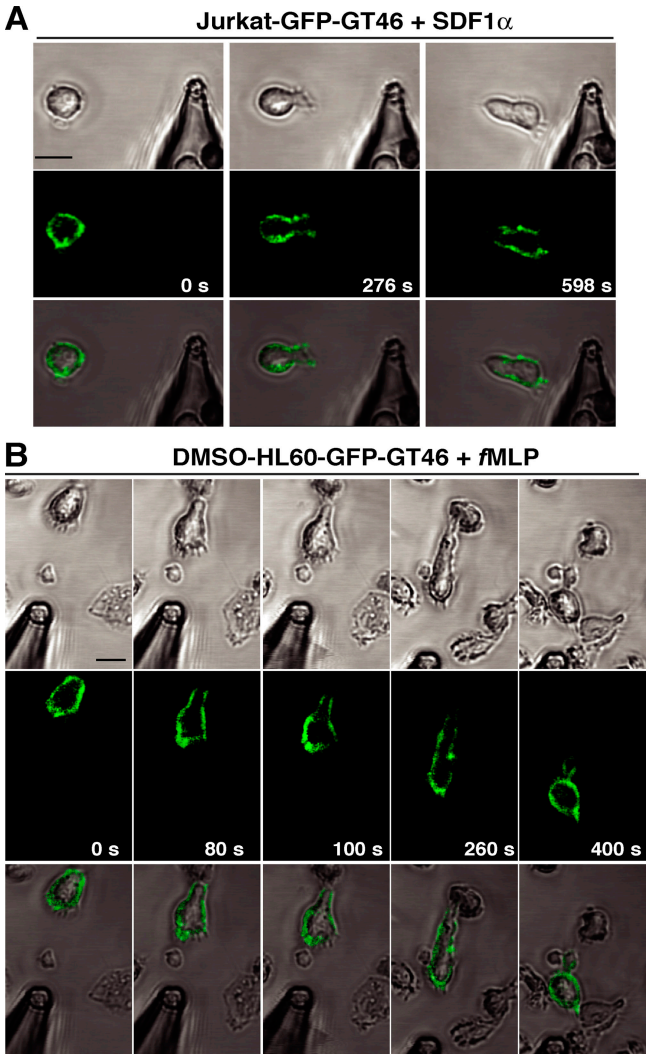

Figure 2. **Nonraft membrane proteins remain evenly distributed during cell chemotaxis.** (A) Jurkat or (B) DMSO-treated HL60 cells expressing the nonraft LGFP-GT46 chimera were analyzed in chemotaxis assays toward an SDF-1α– or an *f*MLP-loaded pipette, respectively, as described in Fig. 1. Confocal images were recorded every 23 s for both cell types. Cells in A and B are representative of 29 of 30 and 32 of 32 cells, respectively; animated versions of these figures are provided as online supplemental material (available at http://www.jcb.org/cgi/content/full/jcb.200309101/DC1). Bars, 10 μm.

labeling redistributed asymmetrically and accumulated in the leading edge and the uropod (Fig. 1, A–C). Raft redistribution in polarized cells occurred shortly after chemoattractant stimulation, persisted in time, and was sensitive to gradient orientation; a change in the position of the attractant-loaded micropipette resulted in rapid GFP-GPI redistribution in the direction of the new chemoattractant source (Fig. 1 C). The use of confocal videomicroscopy minimized variable volume effects, suggesting that asymmetric GFP-GPI redistribution was not the consequence of accumulated fluorescent marker distribution in the z dimension. To verify that lipid raft redistribution is not the consequence of plasma membrane accumulation at these cell locations, GFP-GPI–expressing Jurkat cells were incubated with the fluorescent *FAST*-DiI lipid, which has a preference for nonraft membranes (Seveau et al., 2001). GFP-GPI fluorescence accumulated at the leading edge and at the uropod of SDF-1α–stimulated cells, whereas *FAST*-DiI staining remained largely excluded from these cell areas (Fig. 1 D). These results indicate that raft marker accumulation at these cell sites is not solely the consequence of nonspecific membrane flow.

We also analyzed the dynamic distribution of a nonraft, membrane-anchored GFP-GT46 during chemotaxis in the three cell types. In contrast to the persistent asymmetric GFP-GPI distribution, the nonraft GFP-GT46 protein remained evenly distributed on the surface of Jurkat cells exposed to SDF-1α (Fig. 2 A; Video 4, available at http://www.jcb.org/cgi/content/full/jcb.200309101/DC1) or DMSO-treated HL60 cells exposed to *f*MLP gradients (Fig. 2 B; Video 5). Some GFP-GT46 accumulation was observed at the cell front in certain frames, probably due to membrane flow toward the leading edge. However, after this extension cycle, the GFP-GT46 label was again distributed homogeneously over the cell surface. All together, these results suggest an active mechanism that establishes and maintains asymmetric raft domain distribution in live cells exposed to a local chemoattractant gradient.

L and U raft segregation require chemoattractant-induced actin reorganization

We analyzed the molecular basis of raft redistribution. Treatment of GFP-GPI–expressing Jurkat cells with PTx abolished raft redistribution and morphologic responses to SDF-1α (Fig. 3 A; Video 6, available at http://www.jcb.org/cgi/content/full/jcb.200309101/DC1). This suggested that a PTx-sensitive G_i protein downstream of the CXCR4 receptor mediates L and U raft reorganization. Antibody-induced artificial cross-linking resulted in the formation of large GFP-GPI patches in PTx-treated cells (Fig. 3 B), indicating that PTx treatment does not affect intrinsic raft coalescence. Similar results were obtained for *f*MLP-stimulated differentiated HL60 cells (unpublished data).

Rafts are the preferred cell platforms for membrane-linked actin polymerization and remodeling (Lacalle et al., 2002; Nebl et al., 2002). Cell treatment with latrunculin-B, a toxin that sequesters monomeric actin and causes depolymerization of the actin cytoskeleton, inhibited morphological changes and raft domain redistribution in response to SDF-1α (Fig. 3 C; Video 7, available at http://www.jcb.org/cgi/content/full/jcb.200309101/DC1) or *f*MLP (not depicted). GFP-GPI cross-linking with antibodies caused patch formation on the cell surface (Fig. 3 D), indicating that this treatment does not inhibit raft mobility in the membrane.

Chemoattractant receptors accumulate at the cell front in L rafts

We analyzed whether other raft-associated proteins in addition to GFP-GPI accumulate at the leading edge during chemotaxis. Chemokine receptors are reported to associate with lipid rafts (Mañes et al., 1999, 2000; 2003a; Gómez-Moutón et al., 2001; Sorice et al., 2001; Nguyen and Taub, 2002; Popik et al., 2002; Triantafilou et al., 2002; Viard et al., 2002; Nguyen and Taub, 2003; van Buul et al., 2003; Venkatesan et al., 2003). We constructed GFP-CCR5 chimeras in which the fluorescent protein was tagged to the re-

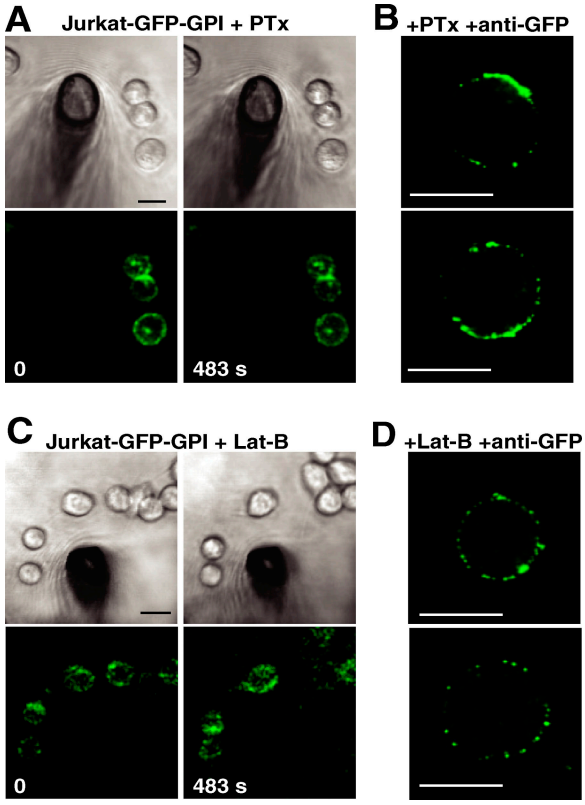

Figure 3. **Raft distribution requires G_i protein signaling and intact actin cytoskeleton.** Chemotaxis assays were performed with GFP-GPI–expressing Jurkat cells treated with PTx (A) or latrunculin-B (C). Only the first and the last time points are shown; animated versions are provided as online supplemental material. Lateral clustering of GFP-GPI in PTx- (B) or latrunculin-B–treated cells (D) was induced by sequential incubation of live cells with anti-GFP and anti–mouse antibodies. Images are representative of 20 of 20 cells were recorded. Bars, 10 μm.

ceptor NH_2 or the COOH terminus. Both chimeras partitioned in L rafts, as indicated by exclusive colocalization with GM3 ganglioside (Fig. 4 A), and responded equally to RANTES (CCL5), as indicated by ligand-induced Ca^{2+} flux (Fig. 4 B). In real-time experiments, we nonetheless found that the COOH terminus GFP-tagged CCR5 chimera internalized in response to ligand and accumulated intracellularly for >60 min (unpublished data), indicating that recycling of this chimera was impaired. This concurs with the observation that the CCR5 COOH terminus is required for appropriate receptor trafficking (Blanpain et al., 2001; Percherancier et al., 2001).

To analyze chemokine receptor redistribution in moving cells, Jurkat cells were cotransfected with the NH_2 terminus–tagged GFP-CCR5 chimera and the AKT PH domain fused to DsRed2-FP (PHAKT-RFP). In Jurkat cells, PHAKT-RFP binds to the membrane in the absence of stimulation (Shan et al., 2000). Thus, PHAKT-RFP may function as a membrane marker able to discriminate between specific protein accumulation at the leading edge and the nonspecific labeling increase due to membrane accumulation at the cell front during chemotaxis. PHAKT-RFP staining was homogeneously distributed in unstimulated cells and concentrated

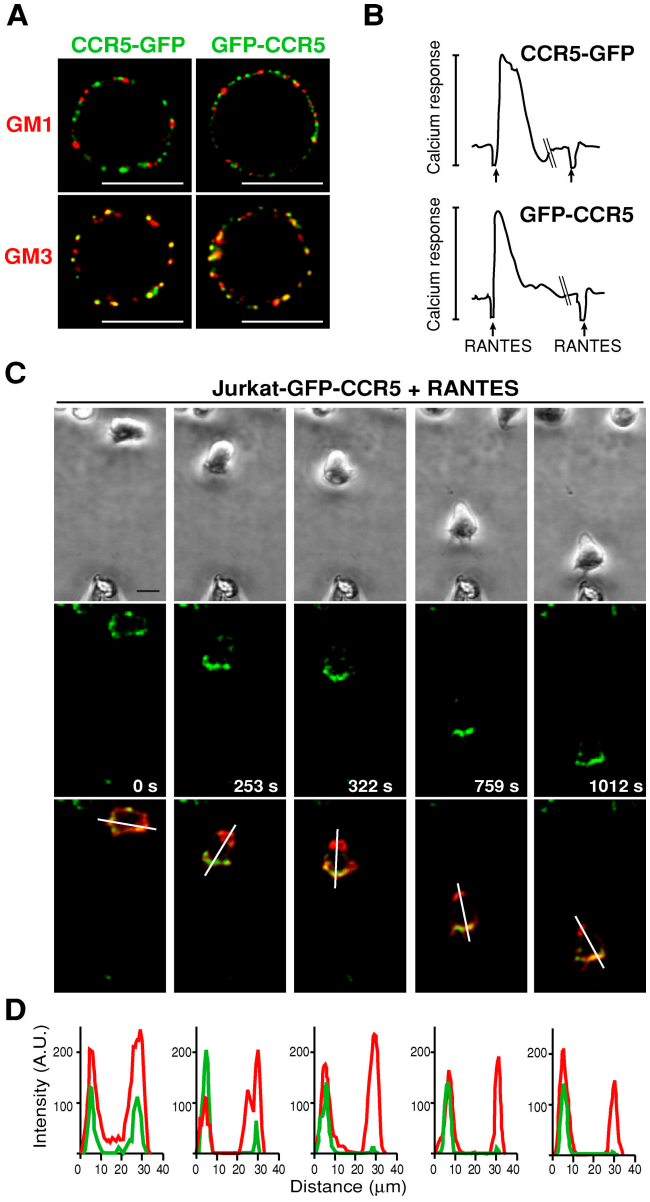

Figure 4. **CCR5 accumulates at the leading edge in L rafts.** (A) Jurkat cells expressing NH_2 or COOH terminus GFP-tagged CCR5 chimeras were incubated with CTx (to detect GM1) or with anti-GM3 antibodies (to detect GM3), and co-patching was performed (see Materials and methods). Images are representative of 29 of 30 cells. Single-color images are provided as online supplemental material (Fig. S2, available at http://www.jcb.org/cgi/content/full/jcb.200309101/DC1). Bars, 10 μm. (B) RANTES-induced Ca^{2+} mobilization in Jurkat cells transfected with the GFP-tagged CCR5 chimera was measured by FACS® analysis. Receptor desensitization was observed after a second RANTES challenge. An ionophore was used to confirm cell loading with Fluo-3,AM (not depicted). (C) Chemotaxis assays toward a RANTES-loaded pipette were performed with GFP-CCR5–expressing Jurkat cells cotransfected with PHAKT-RFP as a plasma membrane marker. Images were recorded in a confocal microscope at 23-s intervals. Dark-phase, green fluorescence, and the merger of red and green channels are shown; an animated version, including single-color recording, is provided as online supplemental material (available at http://www.jcb.org/cgi/content/full/jcb.200309101/DC1). Images are representative of 16 of 20 cells were recorded. (D) Red and green fluorescence scanning of cells in C.

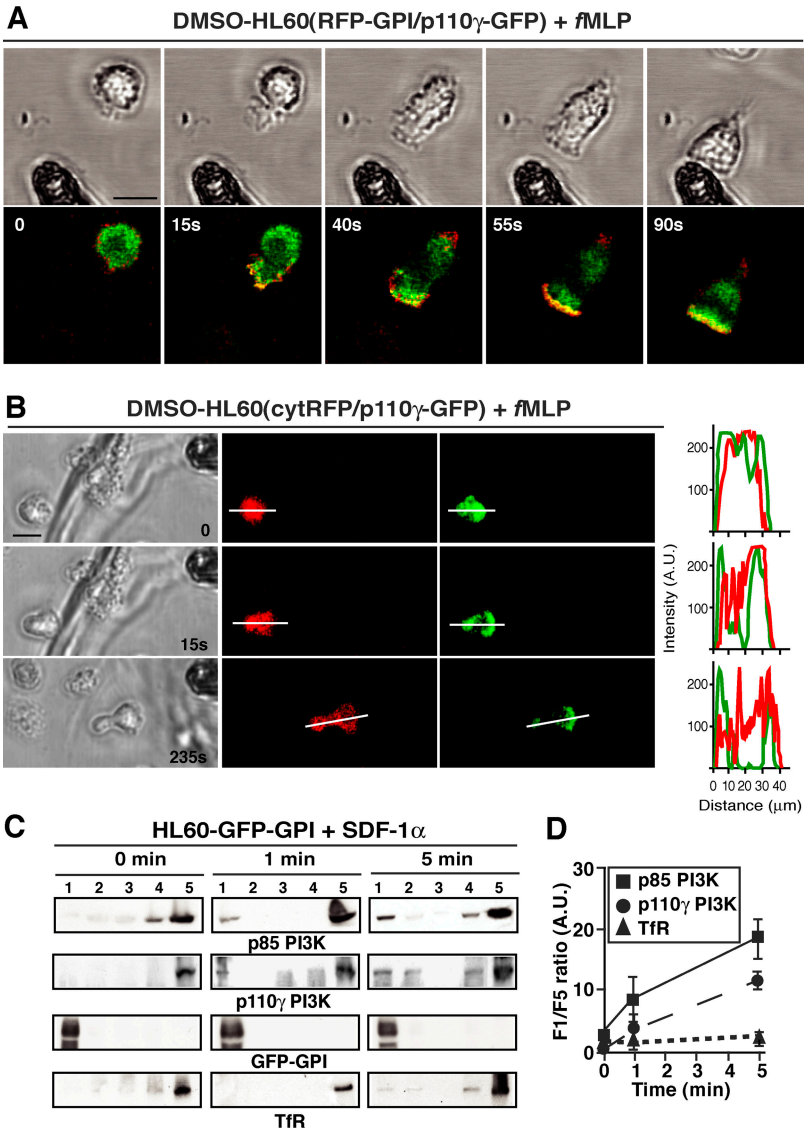

Figure 5. **Chemoattractants induce PI3K recruitment to lipid rafts.** (A) *f*MLP-induced chemotaxis of HL60-DMSO cells coexpressing RFP-GPI (red) and p110γ-GFP (green). The images show dark field and the merger of red and green channels. Images are representative of 13 of 15 cells were recorded. (B) *f*MLP-induced chemotaxis of HL60-DMSO cells coexpressing cytosolic RFP (red) and p110γ-GFP (green). Red and green fluorescence scanning is shown at the right. Images are representative of 12 of 14 cells. In all cases, the first 15 frames were recorded every 5 s and remaining frames every 20 s. Animated versions for A and B, including single-color recording, are provided as online supplemental material (available at http://www.jcb.org/cgi/content/full/jcb.200309101/DC1). Bars, 10 μm. (C) DRM were isolated from unstimulated (0 min) or SDF-1α–stimulated GFP-GPI–expressing HL60 cells by density gradients. Fractions were collected from gradient top (DRM) to bottom (detergent-soluble proteins) and analyzed by Western blot with the indicated antibodies. GFP-GPI and TfR were used as markers for raft- and nonraft-associated proteins, respectively. Similar experiments were performed with *f*MLP-stimulated HL60-DMSO cells (not depicted). (D) The Western blots in C were measured by densitometry, and the intensity ratio between fractions 1 and 5 were calculated for the indicated proteins ($n = 3$). Error bars are SD.

at the front and rear edges when the cell became polarized. In contrast, GFP-CCR5 fluorescence increased persistently only at the leading edge of polarized moving cells (Fig. 4 C; Video 8, available at http://www.jcb.org/cgi/content/full/jcb.200309101/DC1). A scan of fluorescence intensity indicated that the increase in GFP-CCR5 labeling at the cell front in polarized cells is not a consequence solely of the accumulation of highly folded plasma membrane at the leading edge because PHAKT-RFP fluorescence was equivalent between the cell front and rear (Fig. 4 D). This suggests that the GFP-CCR5 fluorescence increase is a consequence of a true increase in receptor density at the leading edge.

Chemoattractant-mediated PI3K recruitment and activation take place in L rafts

Because PI3Kγ (class IB) is activated downstream of the chemokine receptors and is required for neutrophil chemotaxis (Stephens et al., 1997; Wymann and Pirola, 1998; Hannigan et al., 2002), we analyzed whether this isoform is distributed asymmetrically in migrating mammalian cells. Confocal videomicroscopy of DMSO-treated HL60 cells coexpressing RFP-GPI and a COOH-terminal GFP-tagged p110γ PI3K subunit showed that p110γ-GFP is recruited to the cell area facing the *f*MLP source. Leading edge enrichment in p110γ-GFP is closely associated with RFP-GPI redistribution to this site (Fig. 5 A; Video 9, available at http://www.jcb.org/cgi/content/full/jcb.200309101/DC1). Similar experiments performed with cells coexpressing p110γ-GFP and the cytosolic red fluorescent protein (cytRFP) showed that persistent p110γ accumulation at the leading edge is not solely a consequence of the cytoplasm flow that pushes the cell front (Fig. 5 B; Video 10).

Isolation of detergent-resistant membranes (DRM), which are thought to be enriched in raft-associated proteins, showed that chemoattractant stimulation induced p110γ partitioning into DRM (Fig. 5 C). This reinforces the colocalization data with the GPI probe (Fig. 5 A) and supports the idea that PI3K associates to L rafts. Chemoattractant receptors can also activate class IA PI3K in leukocytes (Vicente-Manzanares et al., 1999; Curnock et al., 2003). We were unable to analyze chemoattractant-induced class IA PI3K redistribution, as overexpression of

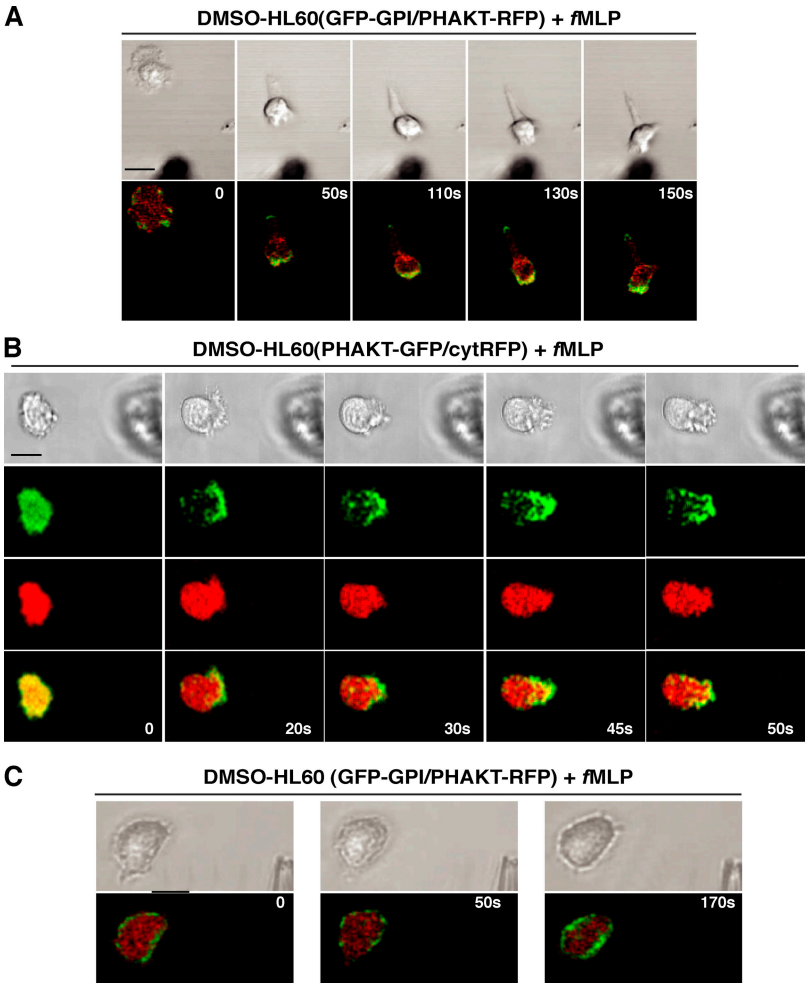

Figure 6. **Attractant-induced PI3K activation parallels L raft redistribution.** (A) *f*MLP-induced chemotaxis of HL60-DMSO cells coexpressing GFP-GPI (green) and PHAKT-RFP (red). Images are representative of 25 of 30 cells. (B) *f*MLP-induced redistribution of PHAKT-GFP (green) in cells coexpressing cytosolic RFP (red). Frames are representative of 14 of 18 cells. (C) HL60-DMSO cells coexpressing GFP-GPI and PHAKT-RFP were treated with 100 μM LY 294002 before *f*MLP-induced chemotaxis. Images are representative of 6 of 10 cells were recorded. Animated versions for A and C, including single-color recording, are provided as online supplemental material (available at http://www.jcb.org/cgi/content/full/jcb.200309101/DC1). Cells were recorded as described in Fig. 5. Bars, 10 μm.

the regulatory p85 subunit produced apoptosis in HL60 and HL60-DMSO cells, even though they were cotransfected with the catalytic p110 subunit. These results stress the importance of a balance in class IA PI3K subunit expression for cell survival (Borlado et al., 2000). Nonetheless, DRM isolation showed that chemoattractant stimulation induced rapid, transient partitioning of class IA PI3K into these microdomains, as indicated by p85 subunit cofractionation with raft-associated GFP-GPI (Fig. 5 C). Similar results were obtained with *f*MLP-stimulated DMSO-HL60 cells (unpublished data). The results suggest that class IA and IB PI3K are recruited from the cytosol to lipid rafts as a consequence of chemoattractant stimulation.

We next analyzed the dynamics of PHAKT-RFP during chemotaxis as an indirect probe for PI3K activation. PHAKT-RFP is recruited mainly to the leading edge of chemotaxing cells (Fig. 6 A; Video 11, available at http://www.jcb.org/cgi/content/full/jcb.200309101/DC1). Coexpression of AKT PH domain fused to GFP (PHAKT-GFP) with cytRFP suggested that a fraction of the PH domain is closely associated to the plasma membrane (Fig. 6 B). Similar results were obtained for undifferentiated SDF-1α–stimulated HL60 cells (unpublished data). Treatment with large doses of the PI3K inhibitor LY294002 abolished PHAKT-RFP recruitment to the leading cell edge, as well as its colocalization with GFP-GPI (Fig. 6 C; Video 12). These results suggest that chemoattractants induce PI3K recruitment and activation in lipid rafts.

Raft redistribution is required for polarization of chemoattractant-associated signaling

To test raft function in PI3K signaling, cells were treated briefly with the cholesterol-sequestering drug methyl-β-cyclodextrin (CD). CD inhibited cell polarization in SDF-1α–stimulated Jurkat (Gómez-Moutón et al., 2001) and *f*MLP-treated HL60-DMSO cells (Fig. 7 A). GFP-GPI was homogeneously distributed on the surface of CD-treated cells exposed to a chemoattractant gradient; likewise, polarized PHAKT-RFP recruitment to the leading edge was not detected in these cells (Fig. 7 B; Video 13, available at http://www.jcb.org/cgi/content/full/jcb.200309101/DC1). CD-treated cells emitted short-lived, randomly directed pseudopodia, independent of the chemoattractant source. Concurrently, arbitrary PHAKT-RFP recruitment to the membrane was observed, suggesting that some degree of chemoattractant receptor signaling is permitted in these cells. These results indicate that CD-treated cells sense the attractant but cannot interpret the gradient. Leading edge accumulation of PHAKT-RFP, redistribution of GFP-GPI and directed cell movement are restored in cholesterol-replenished CD-treated cells (Fig. 7 C; Video 14), indicating that the CD effect was limited to plasma membrane choles-

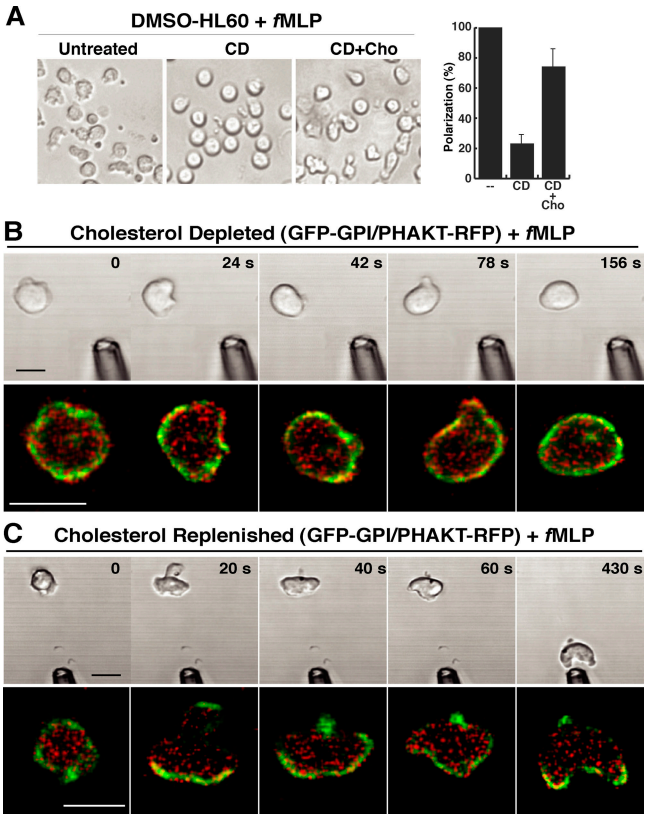

Figure 7. **Gradient sensing in cholesterol-depleted cells.** (A) Differentiated HL60 cells were untreated, cholesterol depleted, or cholesterol replenished before *f*MLP stimulation. Morphological criteria were used to classify polarized cells, which were quantitated in eight fields ($n \approx 100$). The number of polarized cells in untreated conditions was considered 100%. Error bars are SD. (B and C) *f*MLP-induced chemotaxis of (B) cholesterol-depleted and (C) cholesterol-replenished HL60-DMSO cells coexpressing GFP-GPI (green) and PHAKT-RFP (red). Frames were recorded as in Fig. 1. Dark-phase images are shown at a lower magnification to indicate position of the chemoattractant source. Animated versions for B and C, including single-color recording, are provided as online supplemental material (available at http://www.jcb.org/cgi/content/full/jcb.200309101/DC1). Images are representative of (B) 14 of 15 and (C) 11 of 15 cells were recorded. Bars, 10 μm.

terol removal. Coexpression of PHAKT-GFP with the cytosolic RFP probe indicated that the PH domain was partially membrane-associated (unpublished data). These results suggest that membrane domain reorganization is decisive in signal amplification downstream of chemoattractant receptors.

Discussion

The mechanisms used by chemotaxing mammalian cells to restrict the local activation of polarization signals remain largely unknown. Here, we show asymmetric redistribution of raft membrane domains during chemotaxis in living cells. We found that raft domains redistribute to and persist at the leading edge and uropod in directionally stimulated cells. Under similar conditions, a nonraft-associated membrane protein remains homogeneously distributed on the cell surface. The results suggest that raft accumulation at the leading edge and uropod of the polarized chemotaxing cells is due to an active mechanism rather than to membrane flow to cell poles. We also found that raft-associated chemoattractant receptors accumulate actively at the cell front, where they recruit and activate signaling molecules involved in gradient sensing, such as PI3Kγ. Together, the results suggest that membrane rafts function as platforms in which cell polarization signals are elicited and amplified downstream of chemoattractant receptors.

Distinct raft types segregate to the leading edge and uropod in leukocytes

We reported that polarized lymphocytes redistribute GM3-enriched rafts to the leading edge, whereas GM1-based rafts concentrate at the uropod (Gómez-Moutón et al., 2001). This ganglioside segregation is observed in the anterior and posterior parts of HL60 and DMSO-treated HL60 cells (unpublished data). The segregation of distinct raft subtypes to opposite cell poles has been also implicated in pheromone-induced yeast polarization (Bagnat and Simons, 2002), indicating that this complexity is not restricted to leukocytes but probably occurs in many other cell types undergoing polarization. More importantly, we show that persistent L and U raft segregation occurs in live cells engaged in chemotaxis. GFP-GPI colocalizes with GM1 at the uropod and with GM3 at the leading edge (Fig. S1, available at http://www.jcb.org/cgi/content/full/jcb.200309101/DC1), explaining why GFP-GPI labels both cell poles in the time-lapse experiments. Although GFP-GPI has no partitioning bias for a specific raft subtype, there must be molecular signals determining the preferential association of proteins with a specific raft type because the GFP-CCR5 chimera colocalized exclusively with GM3. A possible explanation for this selectivity is that some membrane receptors interact directly with specific lipids, determining their partitioning into specific raft subtypes. For instance, the EGF receptor interacts with GM3 (Miljan et al., 2002) and accumulates at the leading edge during cell electrotaxis (Zhao et al., 2002).

Although our results show GFP-GPI redistribution in all cells studied, relative amounts of this protein vary notably at the front and rear of distinct chemotaxing cell types. Greater GFP-GPI accumulation was observed at the leading edge in Jurkat and in HL60-DMSO cells, whereas undifferentiated HL60 cells showed greater accumulation at the uropod. This variation may reflect the relative size and position of the uropod and the leading edge in these cell types; HL60 cells usually have more prominent uropods than Jurkat or differentiated HL60 cells. These differences may nonetheless represent distinct membrane ganglioside content; HL60 cells have nearly twice as much GM1 as GM3, although this ratio reverses when they are induced to differentiate (Zeng et al., 1995).

Lipid rafts as an organizing platform for signaling during gradient sensing and cell polarization

Current evidence indicates that lipid rafts serve as platforms that increase the efficiency of interactions between activated receptors and signal transduction partners. In migrating cells, lipid rafts may also restrict and/or amplify signaling in specific cell areas. To our knowledge, this paper provides the

first direct evidence of the way in which raft domain segregation controls signaling spatially in mammalian cells engaged in chemotaxis. First, we show that raft-associated proteins, including chemoattractant receptors, polarize to specific cell areas in chemotaxing cells. As demonstrated for GFP-GPI and GFP-CCR5, redistribution of raft-associated proteins does not simply reflect plasma membrane accumulation at the leading edge or the uropod due to membrane folding in those areas. Whereas GFP-CCR5 fluorescence concentrated predominantly at the front of polarized cells, the intensity of a membrane probe was similar at the front and the back of the moving cell. This suggests that GFP-CCR5, as well as other L raft–associated proteins, accumulates and persists at the leading edge via an active mechanism that depends on chemoattractant receptor signaling because PTx suppresses raft redistribution in directionally stimulated cells.

Second, we show that accumulation of the L raft–associated GFP-CCR5 receptor at the cell front correlates with recruitment of the PI3K p110γ catalytic subunit to the leading edge and an increase in PI3K products at this site. Although both p110γ and the AKT PH domain colocalize with the raft probe, we cannot conclude that PI3K activation takes place precisely in L rafts, due to the relatively low resolution of the technique. Nonetheless**,** we also detect recruitment of the class IB and class IA PI3K to DRM after chemoattractant stimulation, again suggesting that PI3K can be activated in rafts. In contrast to PI3K, we did not detect redistribution of both NH_2 and COOH terminus GFP-tagged versions of PTEN (unpublished data).

Finally, we show that cholesterol depletion impedes raft redistribution and, concomitantly, asymmetric PHAKT-RFP recruitment to the cell side facing the chemoattractant source. Chemokine receptor signaling requires association to cholesterol-enriched raft domains (Nguyen and Taub, 2002, 2003). Under the mild cholesterol depletion conditions used here, we observed PH domain recruitment to the membrane, suggesting that G protein–mediated signaling takes place in these cells. The cholesterol-depleted cells can extend small pseudopods, although in random directions; these cells do not recruit PH domains asymmetrically. The results suggest that lipid rafts are involved in cell orientation and polarization toward the attractant source.

We propose that lipid rafts are fundamental elements of the sophisticated guidance system that cells use to orient and move in a chemoattractant gradient. L and U raft segregation permits delivery of "active" receptors to the appropriate cell site, restricting the activation of specific signaling pathways. Our results concur with those of others (Weiner et al., 2002), indicating that signaling molecule relocalization during chemotaxis is the result of interrelated feedback loops. Lipid raft polarization required chemoattractant receptor signaling and actin polymerization, whereas cholesterol depletion prevented asymmetric PI3K activity. Nonetheless, inhibition of PI3K activity also prevented raft redistribution. All these elements would be engaged in positive feedback loops that reinforce the asymmetric sensitivity of the guidance system itself by accumulating chemoattractant receptors at a higher concentration at the cell front. Thus, lipid rafts appear to function as an organizing platform for amplifying intracellular signaling after chemoattractant stimulation.

Materials and methods

Cloning and expression constructs

pGFP-GPI and pGFP-GT46 plasmids were gifts from P. Keller (Max Planck Institute, Dresden, Germany); pRFP-GPI was obtained by subcloning the GPI consensus sequence from pGFP-GPI in pDsRed2-C1 (CLONTECH Laboratories, Inc.). The cDNA encoding the PH domain of AKT (a gift from I. Mérida, CNB, Madrid, Spain) was subcloned in the pDsRed2-C1 or the pEGFP-C1 vector. The p110γ-GFP construct was provided by R. Wetzker (Friedrich-Schiller University, Jena, Germany). To generate the GFP-CCR5 chimera, we cloned the signal peptide from pGFP-GT46 into the pEGFP-C1, followed by four repeats of a serine-glycine spacer and the CCR5 cDNA (a gift from R. Varona, CNB, Madrid, Spain). Jurkat, HL60, and HL60 cells differentiated in the presence of DMSO (HL60-DMSO; 2×10^7 cells) were transfected or cotransfected with the corresponding plasmids by electroporation (250 mV, 975 μF; Bio-Rad Laboratories) or the T Cell Nucleofector Kit (Amaxa Biosystems). Maximum expression was observed 24 h after transfection, as detected by FACS® (Beckman Coulter) and by microscopic analyses. Ficoll density gradients were used to isolate live cells. Cell chemotaxis experiments were performed at 24 h after transfection except in p85-transfected cells, which were used 6 h after transfection to avoid their proapoptotic activity.

Time-lapse confocal videomicroscopy

Real-time cell chemotaxis was studied using time-lapse confocal microscopy. Starved cells were plated for 1 h at 37°C on fibronectin-coated chamber coverslips (Nunc). Cell chemotaxis studies were performed at 37°C using a heating plate and a micromanipulation system (Narishige) adapted to a confocal microscope (Leica). Stimulus was supplied in 1–2 μm of micropipette prepared in a Kopf pipette puller using thin-wall glass capillaries with an inner filament (Clark Electromedical Instruments), filled with 100 nM SDF-1α (PeproTech), 100 nM RANTES (PeproTech) or 100 nM *f*MLP (Sigma-Aldrich) in serum-free RPMI 1640 and sealed at the back. Fluorescence and phase contrast images were recorded at established time intervals and resulting videos were processed with NIH-Image J software. Fluorescence scanning was performed with MicroImage software (Olympus Optical Co.).

In some experiments, starved cells were treated with 10 mM of latrunculin-B for 30 min at 37°C (Calbiochem) or 0.5 μg/ml of PTx for 16 h at 37°C (Sigma-Aldrich), washed twice with medium and plated on fibronectin-coated coverslips for chemotaxis. To inhibit PI3K activity, cells were preincubated with 100 μM of LY 294002 for 1 h (Calbiochem) before plating; LY 294002 was maintained at 40 μM during the chemotaxis assay. To deplete cholesterol, serum-starved cells were treated with 12 mM of CD for 30 min at 37°C (Sigma-Aldrich); CD was removed by washing with serum-free medium containing 0.01% BSA, and an aliquot of CD-treated cells was incubated for 30 min at 37°C in RPMI 1640 containing 100 μg/ml of cholesterol (Sigma-Aldrich) and plated on coverslips for chemotaxis. Dark-phase images were taken from eight fields and cells with a polarized morphology were counted.

Immunofluorescence and antibody-induced patching

Jurkat, HL60, and DMSO-treated HL60 cells were plated on fibronectin-coated chambered glass slides (Nunc) 12 h before assay. Cells were starved and stimulated for 10 min at 37°C with 100 nM SDF-1α or 100 nM *f*MLP, then washed and fixed with 3.7% PFA for 15 min at 20°C in PBS. After fixing, samples were incubated with biotin- or FITC-labeled cholera toxin β-subunit (CTx) for 5 min at 4°C (Sigma-Aldrich) and an anti-GM3 human polyclonal antiserum for 45 min at 4°C (a gift from E. Gallardo and M. Illa, Santa Creu i Sant Pau Hospital, Barcelona, Spain), followed by Cy2- or Cy3-conjugated second antibodies (Jackson ImmunoResearch) or Cy3-streptavidin. In some experiments, Jurkat cells were stained with the di-unsaturated $\Delta^{9,12}$-C_{18} dialkylcarbocyanine (*FAST*-DiI; Molecular Probes) before stimulation with SDF-1α.

For patching experiments, latrunculin-B– or PTx-treated cells were incubated for 30 min at 12°C with an anti-GFP antibody (BD Biosciences). Further cross-linking was performed with Alexa 488–labeled goat anti–mouse antibody for 30 min at 12°C. For co-patching, CCR5-GFP– or GFP-CCR5–expressing Jurkat cells were incubated for 30 min at 12°C with an anti-GFP antibody (CLONTECH Laboratories, Inc.) and biotinylated CTx (Sigma-Aldrich), or with an anti-GM3 antibody. Further cross-linking was performed with the corresponding Cy2- or Cy3-labeled second antibodies. Cells were methanol-fixed for 10 min at −20°C before mounting and confocal analysis.

Calcium determination

Changes in intracellular calcium (Ca^{2+}) concentration were monitored using the fluorescent probe Fluo-3,AM (Molecular Probes). Jurkat cells ex-

pressing the NH_2- or COOH-terminal GFP-tagged CCR5 chimeras were resuspended in RPMI 1640 containing 10% FBS and incubated with Fluo-3,AM (300 mM in DMSO, 10 μl/10^6 cells) for 15 min at 37°C. After incubation, cells were washed and resuspended in complete medium containing 2 mM $CaCl_2$ and maintained at 37°C before addition of 10 nM of RANTES. Ca^{2+} release was determined (37°C, 525 nm) in an EPICS XL flow cytometer (Beckman Coulter).

DRM isolation

DRM were isolated as described previously (Mañes et al., 1999). Normalized protein amounts for each fraction were resolved in SDS-PAGE and analyzed sequentially by blotting with an anti-p85 PI3K (Upstate Biotechnology), an anti-p110 PI3K (a gift from R. Wetzker), anti-GFP, and anti-transferrin receptor (Zymed Laboratories) antibodies.

Online supplemental material

Video 1 shows the dynamic redistribution of GFP-GPI during chemotaxis of Jurkat cells. Video 2 shows the dynamic redistribution of GFP-GPI during chemotaxis of HL60 cells. Video 3 shows the dynamic redistribution of GFP-GPI during chemotaxis of HL60-DMSO cells. Video 4 shows the dynamic redistribution of GFP-GT46 during chemotaxis of Jurkat cells. Video 5 shows the dynamic redistribution of GFP-GT46 during chemotaxis of HL60 cells. Video 6 shows the dynamic redistribution of GFP-GPI in PTx-treated Jurkat cells exposed to an SDF-1α–loaded micropipette. Video 7 shows the dynamic redistribution of GFP-GPI in latrunculin-treated Jurkat cells exposed to an SDF-1α–loaded micropipette. Video 8 shows the dynamic redistribution of GFP-CCR5 and PHAKT-RFP chimeras during chemotaxis of Jurkat cells, including single colors and the merge. Video 9 shows the dynamic redistribution of p110γ-GFP and RFP-GPI during chemotaxis of HL60-DMSO cells. Single colors and the merge are shown. Video 10 shows the dynamic redistribution of p110γ-GFP and cytRFP during chemotaxis of HL60-DMSO cells. Single colors and the merge are shown. Video 11 shows the dynamic redistribution of GFP-GPI and PHAKT-RFP during chemotaxis of HL60-DMSO cells, including single colors and the merge. Video 12 shows the dynamic redistribution of GFP-GPI and PHAKT-RFP during chemotaxis of HL60-DMSO cells pretreated with the PI3K inhibitor LY 294002. Single colors and the merge are shown. Video 13 shows the dynamic redistribution of GFP-GPI and PHAKT-RFP during chemotaxis of HL60-DMSO cells pretreated with methyl-β-CD. Single colors and the merge are shown. Video 14 shows the dynamic redistribution of GFP-GPI and PHAKT-RFP during chemotaxis of methyl-β-CD–treated HL60-DMSO cells replenished with cholesterol. Single colors and the merge are shown. Fig. S1 shows GFP-GPI colocalization with GM3 and GM1 in Jurkat cells. Fig. S2 shows single color images for Fig. 4 A. Online supplemental material is available at http://www.jcb.org/cgi/content/full/jcb.200309101/DC1.

We would like to thank Drs. I. Mérida for the PHAKT vector and for helpful discussions, P. Keller for GFP-GPI and GFP-GT46 expression vectors, R. Wetzker for p110γ-GFP and the anti-p110γ antibody, E. Gallardo and M. Illa for anti-GM3 antiserum, and R. Varona for CCR5 cDNA. We also thank L.M. Criado for help with micromanipulation, M.C. Moreno for cell sorting, and C. Mark for editorial assistance.

S. Jiménez-Baranda is the recipient of a pre-doctoral fellowship from the Spanish Programa de Formación de Personal Universitario. This work was supported by grants from the Spanish MCyT and European Union (QLG1CT 2001-02171). The Department of Immunology and Oncology was founded and is supported by the Spanish Council for Scientific Research (CSIC) and by Pfizer.

Submitted: 16 September 2003
Accepted: 13 January 2004

References

Bagnat, M., and K. Simons. 2002. Cell surface polarization during yeast mating. *Proc. Natl. Acad. Sci. USA.* 99:14183–14188.

Blanpain, C., V. Wittamer, J. Vanderwinden, A. Boom, B. Renneboog, B. Lee, E. Le Poul, L. El Asmar, C. Govaerts, G. Vassart, et al. 2001. Palmitoylation of CCR5 is critical for receptor trafficking and efficient activation of intracellular signaling pathways. *J. Biol. Chem.* 276:23795–23804.

Borlado, L., C. Redondo, B. Alvarez, C. Jimenez, L. Criado, J. Flores, M. Marcos, C. Martinez-A., D. Balomenos, and A. Carrera. 2000. Increased phosphoinositide 3-kinase activity induces a lymphoproliferative disorder and contributes to tumor generation in vivo. *FASEB J.* 14:895–903.

Curnock, A., Y. Sotsios, K. Wright, and S. Ward. 2003. Optimal chemotactic responses of leukemic T cells to stromal cell-derived factor-1 requires the activation of both class IA and IB phosphoinositide 3-kinases. *J. Immunol.* 170: 4021–4030.

Funamoto, S., R. Meili, S. Lee, L. Parry, and R. Firtel. 2002. Spatial and temporal regulation of 3-phosphoinositides by PI3-kinase and PTEN mediates chemotaxis. *Cell.* 109:611–623.

Gómez-Moutón, C., J. Abad, E. Mira, R. Lacalle, E. Gallardo, S. Jiménez-Baranda, I. Illa, A. Bernad, S. Mañes, and C. Martínez-A. 2001. Segregation of leading-edge and uropod components into specific lipid rafts during T cell polarization. *Proc. Natl. Acad. Sci. USA.* 98:9642–9647.

Hannigan, M., L. Zhan, Z. Li, Y. Ai, D. Wu, and C. Huang. 2002. Neutrophils lacking phosphoinositide 3-kinase gamma show loss of directionality during N-formyl-Met-Leu-Phe-induced chemotaxis. *Proc. Natl. Acad. Sci. USA.* 99: 3603–3608.

Iijima, M., and P. Devreotes. 2002. Tumor suppressor PTEN mediates sensing of chemoattractant gradients. *Cell.* 109:599–610.

Katagiri, K., A. Maeda, M. Shimonaka, and T. Kinashi. 2003. RAPL, a Rap1-binding molecule that mediates Rap1-induced adhesion through spatial regulation of LFA-1. *Nat. Immunol.* 4:741–748.

Khanna, K., K. Whaley, L. Zeitlin, T. Moench, K. Mehrazar, R. Cone, Z. Liao, J. Hildreth, T. Hoen, L. Shultz, and R. Markham. 2002. Vaginal transmission of cell-associated HIV-1 in the mouse is blocked by a topical, membrane-modifying agent. *J. Clin. Invest.* 109:205–211.

Lacalle, R., E. Mira, C. Gomez-Mouton, S. Jimenez-Baranda, C. Martinez-A., and S. Mañes. 2002. Specific SHP-2 partitioning in raft domains triggers integrin-mediated signaling via Rho activation. *J. Cell Biol.* 157:277–289.

Lauffenburger, D., and A. Horwitz. 1996. Cell migration: a physically integrated molecular process. *Cell.* 84:359–369.

Mañes, S., E. Mira, C. Gómez-Moutón, R. Lacalle, P. Keller, J. Labrador, and C. Martinez-A. 1999. Membrane raft microdomains mediate front-rear polarity in migrating cells. *EMBO J.* 18:6211–6220.

Mañes, S., G. del Real, R. Lacalle, P. Lucas, C. Gómez-Moutón, S. Sánchez-Palomino, R. Delgado, J. Alcamí, E. Mira, and C. Carlos Martínez-A. 2000. Membrane raft microdomains mediate lateral assemblies required for HIV-1 infection. *EMBO Rep.* 1:190–196.

Mañes, S., G. del Real, and C. Martínez-A. 2003a. Pathogens: raft hijackers. *Nat. Rev. Immunol.*:557–568.

Mañes, S., R. Ana Lacalle, C. Gómez-Moutón, and C. Martínez-A. 2003b. From rafts to crafts: membrane asymmetry in moving cells. *Trends Immunol.* 24: 320–326.

McKay, D., J. Kusel, and P. Wilkinson. 1991. Studies of chemotactic factor-induced polarity in human neutrophils. Lipid mobility, receptor redistribution and the time-sequence of polarization. *J. Cell Sci.* 100:473–479.

Miljan, E., E. Meuillet, B. Mania-Farnell, D. George, H. Yamamoto, H. Simon, and E. Bremer. 2002. Interaction of the extracellular domain of the epidermal growth factor receptor with gangliosides. *J. Biol. Chem.* 277:10108–10113.

Millan, J., M. Montoya, D. Sancho, F. Sanchez-Madrid, and M. Alonso. 2002. Lipid rafts mediate biosynthetic transport to the T lymphocyte uropod subdomain and are necessary for uropod integrity and function. *Blood.* 99:978–984.

Nebl, T., K. Pestonjamasp, J. Leszyk, J. Crowley, S. Oh, and E. Luna. 2002. Proteomic analysis of a detergent-resistant membrane skeleton from neutrophil plasma membranes. *J. Biol. Chem.* 277:43399–43409.

Nguyen, D., and D. Taub. 2002. CXCR4 function requires membrane cholesterol: implications for HIV infection. *J. Immunol.* 168:4121–4126.

Nguyen, D., and D. Taub. 2003. Inhibition of chemokine receptor function by membrane cholesterol oxidation. *Exp. Cell Res.* 291:36–45.

Nieto, M., J. Frade, D. Sancho, M. Mellado, C. Martínez-A., and F. Sánchez-Madrid. 1997. Polarization of chemokine receptors to the leading edge during lymphocyte chemotaxis. *J. Exp. Med.* 186:153–158.

Percherancier, Y., T. Planchenault, A. Valenzuela-Fernandez, J. Virelizier, F. Arenzana-Seisdedos, and F. Bachelerie. 2001. Palmitoylation-dependent control of degradation, life span, and membrane expression of the CCR5 receptor. *J. Biol. Chem.* 276:31936–31944.

Popik, W., T. Alce, and W. Au. 2002. Human immunodeficiency virus type 1 uses lipid raft-colocalized CD4 and chemokine receptors for productive entry into CD4(+) T cells. *J. Virol.* 76:4709–4722.

Pralle, A., P. Keller, E.L. Florin, K. Simons, and J.K. Hörber. 2000. Sphingolipid-cholesterol rafts diffuse as small entities in the plasma membrane of mammalian cells. *J. Cell Biol.* 148:997–1008.

Servant, G., O. Weiner, E. Neptune, J. Sedat, and H. Bourne. 1999. Dynamics of

a chemoattractant receptor in living neutrophils during chemotaxis. *Mol. Biol. Cell.* 10:1163–1178.

Servant, G., O. Weiner, P. Herzmark, T. Balla, J. Sedat, and H. Bourne. 2000. Polarization of chemoattractant receptor signaling during neutrophil chemotaxis. *Science.* 287:1037–1040.

Seveau, S., R. Eddy, F. Maxfield, and L. Pierini. 2001. Cytoskeleton-dependent membrane domain segregation during neutrophil polarization. *Mol. Biol. Cell.* 12:3550–3562.

Shan, X., M. Czar, S. Bunnell, P. Liu, Y. Liu, P. Schwartzberg, and R. Wange. 2000. Deficiency of PTEN in Jurkat T cells causes constitutive localization of Itk to the plasma membrane and hyperresponsiveness to CD3 stimulation. *Mol. Cell. Biol.* 20:6945–6957.

Sorice, M., T. Garofalo, R. Misasi, A. Longo, V. Mattei, P. Sale, V. Dolo, R. Gradini, and A. Pavan. 2001. Evidence for cell surface association between CXCR4 and ganglioside GM3 after gp120 binding in SupT1 lymphoblastoid cells. *FEBS Lett.* 506:55–60.

Stephens, L., A. Eguinoa, H. Erdjument-Bromage, M. Lui, F. Cooke, J. Coadwell, A. Smrcka, M. Thelen, K. Cadwallader, P. Tempst, and P. Hawkins. 1997. The G beta gamma sensitivity of a PI3K is dependent upon a tightly associated adaptor, p101. *Cell.* 89:105–114.

Sullivan, S., G. Daukas, and S. Zigmond. 1984. Asymmetric distribution of the chemotactic peptide receptor on polymorphonuclear leukocytes. *J. Cell Biol.* 99:1461–1467.

Triantafilou, M., K. Miyake, D. Golenbock, and K. Triantafilou. 2002. Mediators of innate immune recognition of bacteria concentrate in lipid rafts and facilitate lipopolysaccharide-induced cell activation. *J. Cell Sci.* 115:2603–2611.

van Buul, J., C. Voermans, J. van Gelderen, E. Anthony, C. van der Schoot, and P. Hordijk. 2003. Leukocyte-endothelium interaction promotes SDF-1-dependent polarization of CXCR4. *J. Biol. Chem.* 278:30302–30310.

Venkatesan, S., J. Rose, R. Lodge, P. Murphy, and J. Foley. 2003. Distinct mechanisms of agonist-induced endocytosis for human chemokine receptors CCR5 and CXCR4. *Mol. Biol. Cell.* 14:3305–3324.

Viard, M., I. Parolini, M. Sargiacomo, K. Fecchi, C. Ramoni, S. Ablan, F. Ruscetti, J. Wang, and R. Blumenthal. 2002. Role of cholesterol in human immunodeficiency virus type 1 envelope protein-mediated fusion with host cells. *J. Virol.* 76:11584–11595.

Vicente-Manzanares, M., M. Rey, D. Jones, D. Sancho, M. Mellado, J. Rodríguez-Frade, M. del Pozo, M. Yáñez-Mo, A.M. de Ana, C. Martínez-A, et al. 1999. Involvement of phosphatidylinositol 3-kinase in stromal cell-derived factor-1 alpha-induced lymphocyte polarization and chemotaxis. *J. Immunol.* 163:4001–4012.

Walter, R., and W. Marasco. 1984. Localization of chemotactic peptide receptors on rabbit neutrophils. *Exp. Cell Res.* 154:613–618.

Weiner, O.D., P.O. Neilsen, G.D. Prestwich, M.W. Kirschner, L.C. Cantley, and H.R. Bourne. 2002. A PtdInsP(3)- and Rho GTPase-mediated positive feedback loop regulates neutrophil polarity. *Nat. Cell Biol.* 4:509–513.

Wymann, M., and L. Pirola. 1998. Structure and function of phosphoinositide 3-kinases. *Biochim. Biophys. Acta.* 1436:127–150.

Zeng, G., T. Ariga, X.-B. Gu, and R. Yu. 1995. Regulation of glycolipid synthesis in HL-60 cells by antisense oligodeoxynucleotides to glycosyltransferase sequences: effect on cellular differentiation. *Proc. Natl. Acad. Sci. USA.* 92: 8670–8674.

Zhao, M., J. Pu, J. Forrester, and C. McCaig. 2002. Membrane lipids, EGF receptors, and intracellular signals colocalize and are polarized in epithelial cells moving directionally in a physiological electric field. *FASEB J.* 16:857–859.